

2 Monometallic Benzo[*b*]thienyl-carbene Complexes

1. Introduction

Benzo[*b*]thiophene

The first example of a carbene metal complex containing an aromatic substituent is coincidentally also the first reported carbene complex $[\text{W}(\text{CO})_5\text{C}(\text{OMe})\text{Ph}]$ prepared by Fischer and Maasböl.¹ After refining the synthetic process² they concluded that these carbene complexes are generally quite stable, diamagnetic, soluble in organic solvents, and sublimable. A compound like **G** (Scheme 1.2) is of this kind and contains a single metal-fragment. Benzo[*b*]thiophene (BT) is an example of a heteroarene and has a benzene ring fused to a thiophene ring. Since the 1960s it was agreed that aromatic compounds have the following characteristics:³

- (I) They have cyclic delocalized π -electron systems and are planar.
- (II) They are more stable than their olefinic analogues by an energy called the resonance energy.
- (III) Bond lengths between adjacent atoms intermediate between those of typical single and double bonds.
- (IV) They have a π -electron ring current induced by an external magnetic field, leading to increased diamagnetic susceptibility and typical diatropic [low field] chemical shifts of exocyclic protons in ^1H NMR spectra.
- (V) Substitution reactions take place more readily than addition reactions.
- (VI) Spectroscopically they show higher energy ultraviolet/visible spectral bands and a more symmetrical structure for their IR spectra.

It is important to note that heterocycles can be classified as π -excessive or π -deficient. π -Excessive heterocycles are compounds in which the number of π -electrons in the conjugated system exceeds the number of atoms forming the cycle. The compounds pyrrole, thiophene, benzo[*b*]thiophene, indole and dibenzothiophene are classical examples of π -excessive heterocycles. In this chapter focus falls on carbene complexes containing BT, of which the molecular orbital calculations of the localized charges for each of the carbon atoms and the sulphur atom have been reported.⁴

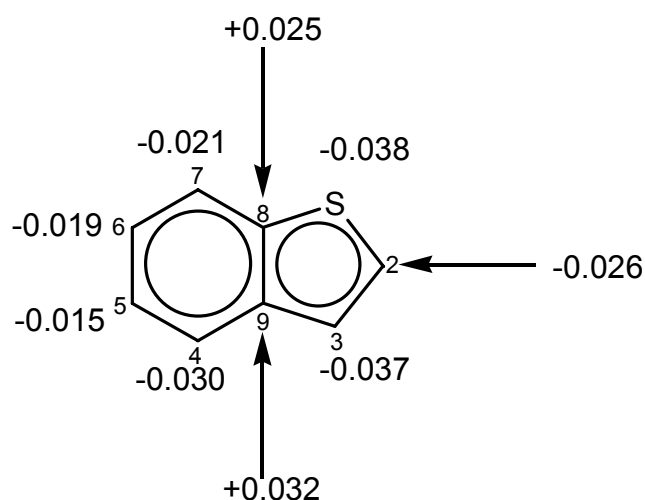


Figure 2.1 Molecular orbital charge calculations and atom numbering for benzo[*b*]thiophene

Molecular orbital calculations for BT have revealed that the highest electron densities are on the sulphur and the C2-C3 carbon atoms, giving rise to the fact that BT is easily deprotonated in high yields in the 2-position of the thiophene ring to give benzothieryllithium. This lithiated precursor can be used to react with transition metal hexacarbonyls.

Stabilization of carbene complexes

A complete study has been conducted on complexes of the type $[M(CO)_5C(X)Y]$, where M = Cr or W; X = OR or NR^1R^2 , and Y is an organic group, with the aid of NMR spectroscopy. The findings were that the chemical shift of the carbene carbon is more strongly influenced by X than by either M or Y.⁵ Mills in cooperation with Fischer and his

co-workers carried out a single crystal X-ray structure determination of the carbene complex, pentacarbonyl[methoxy-(phenyl)carbene]-chromium(0).⁶ This structure confirmed that the carbene carbon atom is sp^2 hybridized, which also indicates an empty p -orbital and an electron-deficient carbon atom.

There are three ways in which the electron deficiency on the carbene carbon atom can be relieved and the carbene complex stabilized. This can be achieved mainly by π -interaction from the substituents with π -bonding facilities. Carbene stabilization is predominantly from the low oxidation state metal and/or from the heteroatom lone pair bonded to the carbene carbon. A $p\pi-p\pi$ bond can form between one of the lone electron pairs on the oxygen atom of the alkoxy group and the unused p -orbital of the carbene carbon. In amino carbene complexes this effect is even enhanced to such an extent that geometric isomers exist and can be isolated.⁷ Also very important is $d\pi-p\pi$ backbonding from occupied central metal (tungsten or chromium) orbitals to the empty p -orbital of the carbene carbon. It is known that the carbonyl ligands in metal-carbonyl complexes may be considered as weak σ -donor and good π -acceptor ligands. This represents a synergic σ -donor and π -acceptor bonding mode and increases the metal-carbon(carbonyl) bond order. Compared to carbonyl ligands, Fischer carbene ligands are stronger σ -donor but weaker π -acceptor ligands. However, the role of the third substituent to π -stabilize the carbene carbon atom *via* $p\pi-p\pi$ interaction could also be important if the substituent is an aryl. This electron withdrawing effect should be comparable to the effect observed of an ester substituent on an aryl-type ring with a conjugated π -system. Connor and Jones studied the role of the heteroatom in heteroarene substituted carbene complexes.⁸ It was assumed that by changing the heteroatom (Figure 2.2) in the heteroarene substituent, the contribution of π -stabilization of the carbene carbon by this substituent should differ.

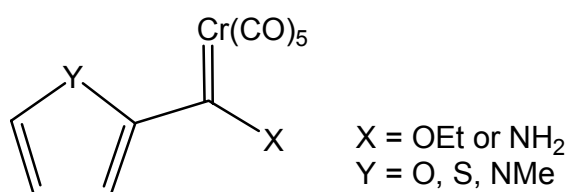


Figure 2.2 A heteroarene substituent with different heteroatoms in carbene complexes⁸

It was found that the heteroarene rings will π -donate electron density to the carbene carbon and the effect will increase in the order $Y = O < S < NMe$.

In this study the effect of carbene stabilization by all three substituents comes under scrutiny. In this chapter the carbene complexes shown in Figure 2.3 were synthesized and characterized. The carbene carbon is in π -contact with the benzo[*b*]thiophene substituent and the oxygen substituent.

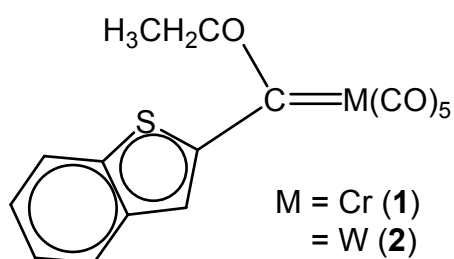
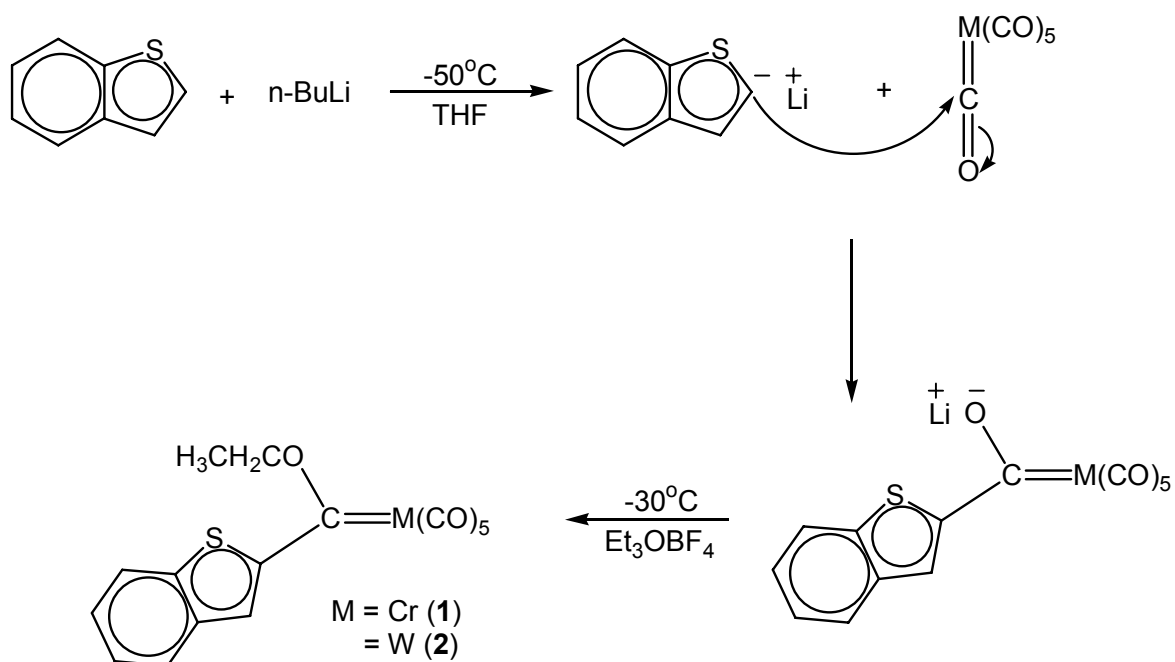


Figure 2.3 Carbene complexes synthesized in this chapter

To study electronic and steric properties in solution, spectroscopic measurements were recorded and in the solid-state crystal structure determinations were performed. Although **1** and **2** represent fairly simple examples of Fischer carbene complexes, they form the basis and reference point of a systematic study of di- and trimetallic carbene complexes. It is reasonable to assume that benzothienyl substituents should be comparable to thienyl substituents in their potential to donate electron density to the carbene carbon. Fischer carbene complexes with thienyl substituents have been prepared and studied before.⁸⁻¹⁰

2. Metallation

Deprotonation of BT is accomplished by the use of a strong base ($pK_a > 20$) e.g. *n*-BuLi (*n*-butyllithium). The acidity of the arene protons allows hydrogen-metal exchange to occur on the 2-position, in the thiophene ring, under conditions as specified (Scheme 2.1).



Scheme 2.1

The metallated BT has nucleophilic properties located on the α -carbon of the thiophene ring and attacks an electron deficient carbon atom belonging to the metal hexacarbonyl complex to form a metal acylate. After replacing the solvent with dichloromethane, triethyloxonium salt was added to the metal acylate and the desired neutral carbene complexes formed. The formation of the carbene complexes, **1** (red) and **2** (red-brown), occurred with high yields and the complexes were purified with column chromatography, using silica gel as stationary phase.

3. Spectroscopic characterization

The carbene complexes **1** and **2** were characterized in solution using NMR and infrared spectroscopy and in the solid state by molecular crystal structure determinations.

3.1 NMR Spectroscopy

The chemical shift values of ligand nuclei are affected when coordination of a metal fragment occurs. The resulting coordination shift, defined as the chemical shift difference between the metal bonded ligand and the free ligand is indicated with the symbol $\Delta\delta$.

3.1.1 ^1H NMR spectroscopy

The signals in the ^1H NMR spectrum of uncoordinated BT were resolved and a full iterative analysis was carried out.¹¹ The signals of the protons of BT in deuterated chloroform are given in Figure 2.4.^{12,13} and the following system of numbering of the protons and carbon atoms of benzo[*b*]thiophene will be used throughout the whole discussion.

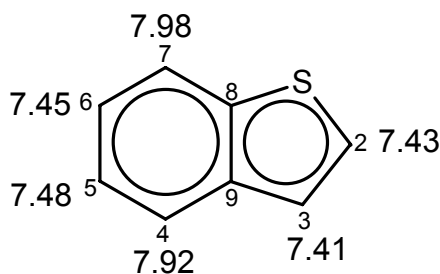


Figure 2.4 Chemical shifts of the protons of BT and atom labelling used for benzo[*b*]thiophene complexes

^1H NMR spectra were recorded in CDCl_3 as well as C_6D_6 as reported in Table 2.1, the assignment of the chemical shifts to the individual protons was resolved from chemical shift values and a HETCOR experiment along with the chemical shift values obtained for the starting material. In complexes **1** - **2**, the singlet of coordinated BT, (or doublet due to long distance coupling) and the doublet of uncoordinated BT observed for the thienyl protons along with the coupling constants and patterns, prove that the carbene carbon is bonded at the 2-position of the BT ligand. Since H3 is the proton closest to the site of coordination to the metal fragment, the chemical shift of this proton is influenced the most.

Comparing the data of uncoordinated BT (Figure 2.5) with the data of BT in compounds **1** and **2**, it is evident that the metal-fragment and metal type have a significant influence on the ring protons. By comparing only the CDCl_3 values, since the ^1H NMR spectrum of the uncoordinated BT was only in CDCl_3 , it is evident that a large down field chemical shift ($\Delta\delta \approx 1$ ppm) for H3 occurs. This is expected due to the electron withdrawing character of the carbene carbon bonded to the 2-position of the BT ring as well as the coordination of the carbene carbon to the $\text{M}(\text{CO})_5$ fragment. As a result the withdrawal of electron density from the 3-position was observed, leading to a more deshielded proton, and causing a downfield chemical shift.

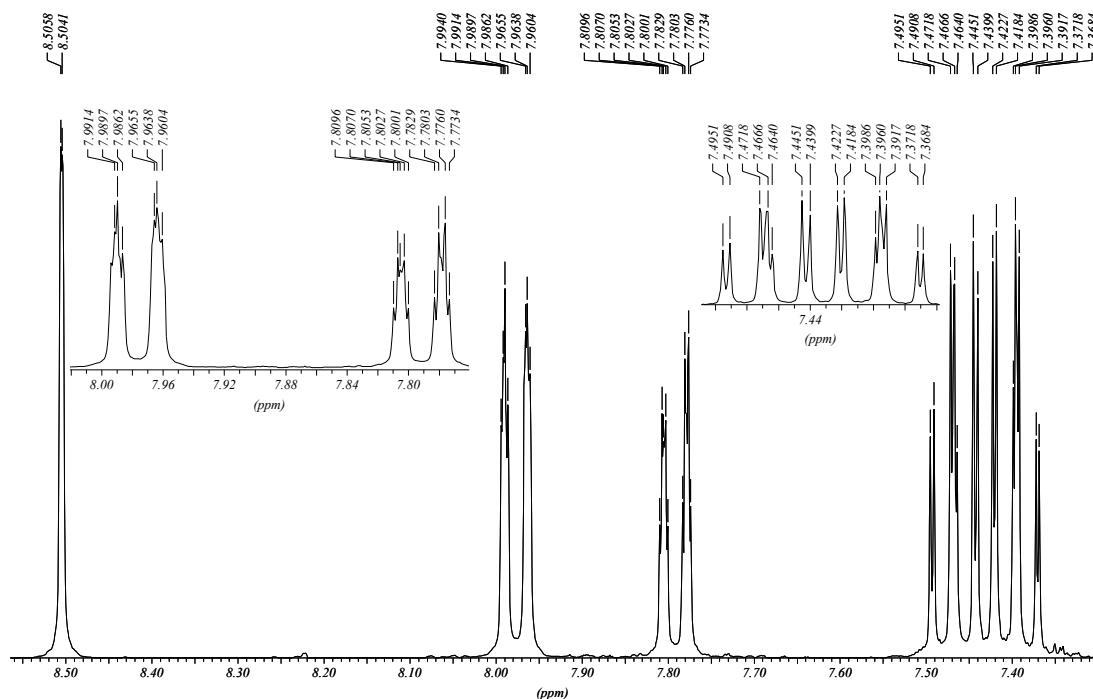
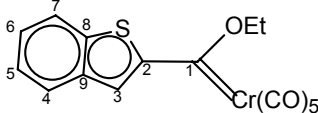
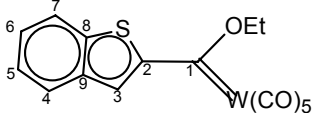


Figure 2.5 ^1H NMR spectrum of complex **1** in CDCl_3 , in the region for the ring protons

When comparing compounds **1** and **2**, one can recognise a more deshielded H3 proton for complex **1** ($\Delta\delta \approx 0.1$ ppm). The methylene protons of the etoxycarbene substituent are also downfield for **1** compared to **2** ($\Delta\delta \approx 0.2$ ppm). This is ascribed to the different metals bonded to the carbene carbon. Interestingly, the benzene protons H4-H7 are little affected compared to the thiophene proton, indicating that little charge is withdrawn from the benzene ring.

Problems were experienced during the effort to determine the coupling constant of the H5-H6 signal due to the overlap of the NMR signals, and no value could be assigned unambiguously. Coupling constants of H5 and H6 to protons H4 and H7 were resolved with the help from the resolutions obtained from the H4 and H7 proton signals, which had clear coupling constants.

Table 2.1 ^1H NMR data of complexes **1** and **2**

Assignment	Complexes				
	Chemical shifts (δ , ppm) and coupling constants (J, Hz)				
	 1			 2	
Proton	δ	$^3J_{\text{H-H}}$	$^4J_{\text{H-H}}$	δ	$^3J_{\text{H-H}}$
H3 ^a	8.50 (d)	-	0.8	8.39 (s)	-
H4	7.80 (dddd)	8.0	1.8 0.8	7.79 (d)	8.2
H5	7.47 (ddd)	8.0	1.03	7.50 (m)	8.2
H6	7.40 (ddd)	7.8	1.8	7.39 (m)	7.9
H7	8.00 (dd)	7.8	1.03	8.00 (d)	7.9
-CH ₂ -	5.25 (q)	7.0	-	5.04 (q)	6.9
-CH ₃	1.72 (t)	7.0	-	1.69 (t)	6.9
H3 ^b	8.51 (s)	-	-	8.40 (s)	-
H4	7.33 (d)	7.9	-	7.31 (dd)	8.1
H5	7.00 (t)	7.9	-	7.01 (m)	8.1
H6	6.95 (t)	7.9	-	6.94 (m)	8.1
H7	7.46 (d)	7.9	-	7.45 (d)	8.1
-CH ₂ -	4.70 (q)	6.9	-	4.51 (q)	7.0
-CH ₃	1.05 (t)	6.9	-	1.02 (t)	7.0

^a spectrum was recorded in CDCl₃^b spectrum was recorded in C₆D₆

3.1.2 ^{13}C NMR spectroscopy

The chemical shifts in the ^{13}C NMR spectrum of uncoordinated BT in deuterated chloroform are known from literature¹¹⁻¹³ and are as follow: 126.1 (C2), 123.7 (C3) 139.5, 134.6 (C8, C9), 123.5 (C4), 124.0 (C5), 124.1 (C6), 122.3 (C7).

The ^{13}C NMR data of complexes **1** and **2** are summarized in Table 2.2 and the chemical shift values were assigned with the help of the information gained from a 2D HETCOR experiment. Due to poor solubility in C_6D_6 , the ^{13}C NMR spectrum of compound **1** does not show all the resonances.

Table 2.2 ^{13}C NMR chemical shifts of complexes **1** and **2**

Assignment	Complexes			
	Chemical shifts (δ , ppm)			
	1		2	
Carbon	δ^a	δ^b	δ^a	δ^b
C1	320.5	320.2	294.3	294.2
C2	154.0	-	157.0	157.5
C3	141.9	139.5	142.5	143.2
C4	122.8	122.7	122.9	122.9
C5	128.9	129.1	128.8	129.0
C6	125.1	125.2	125.2	125.4
C7	126.8	128.6	126.9	127.1
C8, C9	138.7, 139.2	-	139.0, 139.5	139.3, 139.7
-CH ₂ -	76.5	76.6	79.0	79.1
-CH ₃	15.1	14.5	14.9	14.3
CO	216.9 (cis) 223.4 (trans)	217.4 (cis) 223.8 (trans)	197.5 (cis), (sattelites) 202.6 (trans)	197.9 (cis), (sattelites) 203.1 (trans)

^a spectrum was recorded in CDCl_3

^b spectrum was recorded in C_6D_6

Notable differences are observed when comparing the ^{13}C NMR chemical shift values of the uncoordinated BT with those of the complexes **1** and **2**. It is obvious that the thiophene

ring, where the carbene carbon is attached (C2) and other thiophene carbons (C3,C8,C9), are more affected than those of the benzene ring fragment. Again, this is due to the electron withdrawing effect of the carbene carbon C1 and charge delocalization of the thiophene ring, which in itself has the highest down field chemical shift due to electron deficiency. In free BT charge delocalization is mostly within the thiophene ring with a resulting shielding effect. When BT is attached to a carbene carbon atom, delocalization is outwards towards the carbene carbon with a resulting deshielding effect.

For both compounds the $M(CO)_5$ resonances are depicted as two signals of different intensities, indicating a difference in chemical shifts of the CO carbons. This is due to the fact that one carbonyl is *trans* to the carbene ligand where the other four ligands are found *cis* to the carbene carbon or opposite carbonyl ligands. The interesting pattern observed at 197.5 ppm in $CDCl_3$ and 197.9 ppm in C_6D_6 , for the *cis* carbonyl resonance of complex **2** (Figure 2.6), is ascribed to $^{13}C-^{183}W$ coupling ($J = 63.3$ Hz). Other examples of $^{13}C-^{183}W$ coupling have been reported.¹⁴

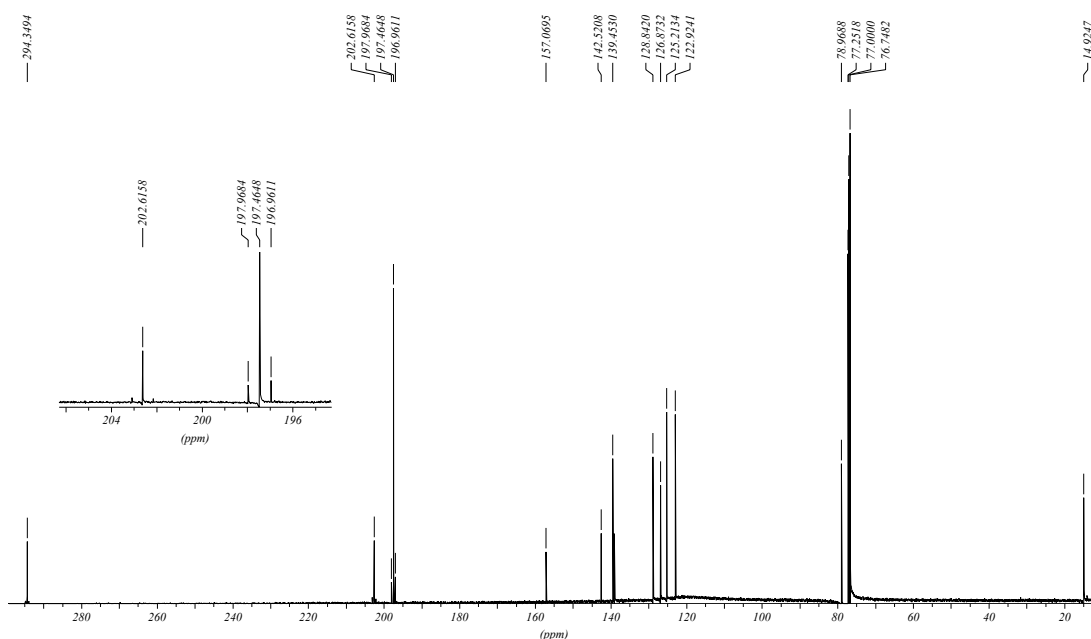


Figure 2.6 ^{13}C NMR spectrum in $CDCl_3$ of complex **2** with the enlarged CO region

3.1.3 2D HETCOR Experiment

In this experiment one-bond ^1H - ^{13}C couplings are used to show directly which protons are attached to which carbon atoms. In Figure 2.7 the HETCOR spectra of complex **2** is represented. The chemical shifts of H (δ_{H}) are stipulated on the x-axis, while the chemical shifts of C (δ_{C}) are introduced on the y-axis. From this data it was possible to assign C3, C4-C7 to the corresponding protons in ^1H NMR spectrum.

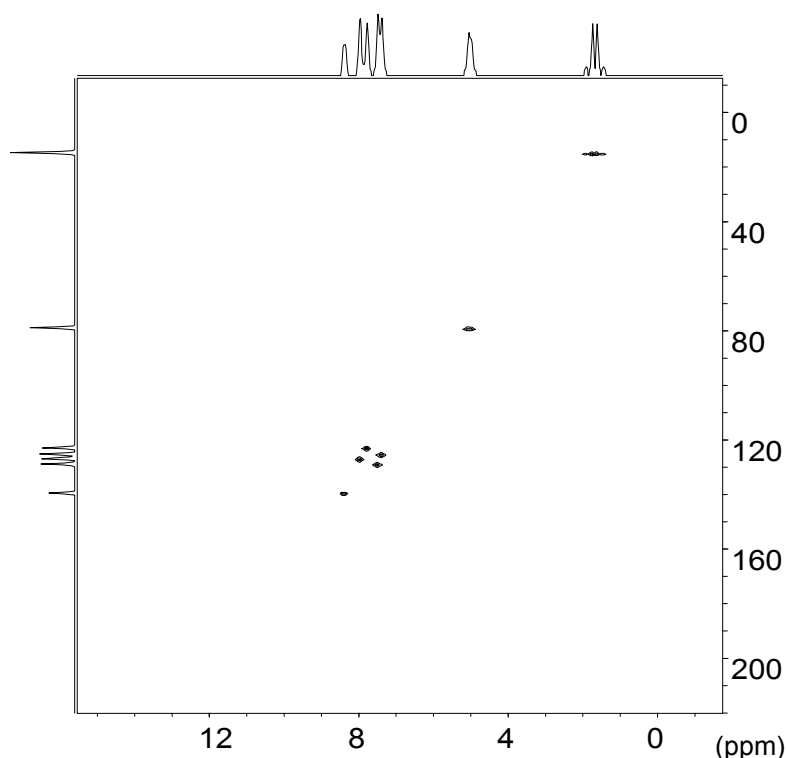


Figure 2.7 2D HETCOR spectrum of compound **2**

3.2 Infrared Spectroscopy

A lot of structural and electronic information of ligands can be obtained from the infrared spectra in the carbonyl region of metal carbonyl complexes. The transition metal-CO bond of a terminal carbonyl ligand is described as a resonance hybrid and the bond order for the M-C and C-O bonds are determined by the electronic properties of the metal and other ligands in the compound. The bond order for the M-C bond can either be 1 (a) or 2 (b) and the bond order for the C-O bond varies accordingly from 3 (a) to 2 (b) as seen in figure 2.8.

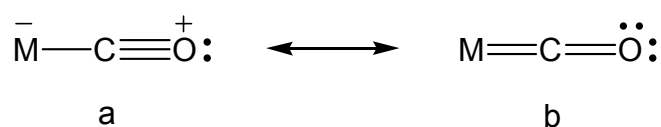


Figure 2.8 Resonance structures for the M-C-O bonds in metal carbonyl complexes

The resonance effect observed in **a** is due to the electron density donation from the carbonyl ligand to the metal *via* a σ -donor interaction. In return, the metal can donate electron density to the carbonyl *via* π -interaction (backbonding) shown by **b**. The magnitude of the backbonding depends on the nature of the transition metal and other non-carbonyl ligands. Obviously when late transition metals are concerned or complexes have a net negative charge, backbonding will play a decisive role, since the electron density on these metals are considerably higher than for early transition metals. C-O stretching vibrational frequencies can be regarded as being independent from other vibrations in the molecule, thus a qualitative correlation between CO stretching vibrational frequencies and the bond order of the C-O bond can be made.¹⁵ As backbonding from the metal to the carbonyl ligand increases, the M-C bond becomes stronger and thus shorter. The C-O bond weakens accordingly and becomes longer. This increase in bond order of the M-C bond, prompts the carbonyl stretching frequency to shift to a lower wavenumber on the IR spectrum.

The number and intensities of carbonyl stretching frequencies are dependent on the local symmetry of the carbonyl ligands around the central atom. According to the method of local symmetry¹⁶ a pentacarbonyl complex of the type $\text{M}(\text{CO})_5\text{L}$, belongs to the symmetry group C_{4v} , which can perform four vibrations namely $\text{A}_1^{(1)}$, $\text{A}_1^{(2)}$, B_1 and E. As seen in Figure 2.9, only two vibrational bands are IR active and they are the E and $\text{A}_1^{(2)}$ bands, the other bands can be detected with Raman spectroscopy, however the $\text{A}_1^{(1)}$ band may become IR active due to coupling with the vibrational modes of the $\text{A}_1^{(2)}$ band vibrations and since complexes in discussion do not exhibit absolute C_{4v} symmetry, distortions in the carbonyl plane are possible, resulting in an IR-active B_1 band. Aspects related to tricarbonyl fragments will be discussed in Chapter 4.

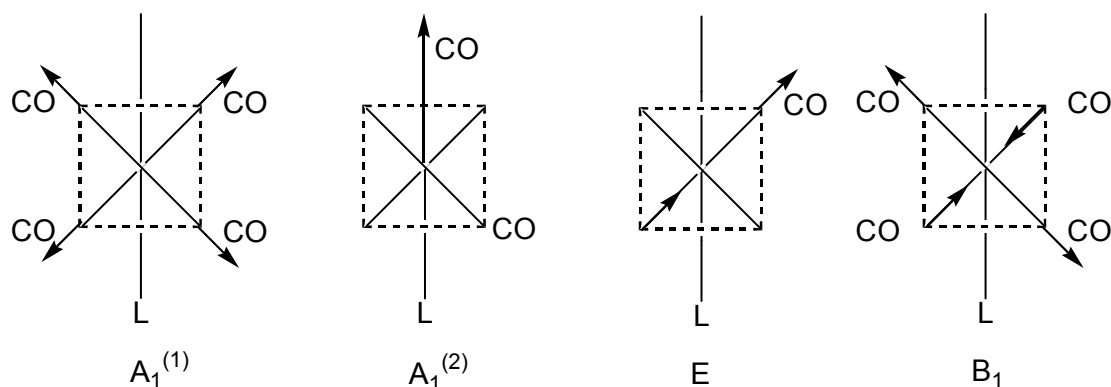


Figure 2.9 Stretching vibration modes of $[M(CO)_5L]$ complexes

From Figure 2.9 it is clear that the $A_1^{(2)}$ and the E bands will display the highest intensities on the IR spectrum. The $A_1^{(2)}$ band is often observed as a "shoulder" on the spectrum, at the higher frequency side of the E band when the unique ligand is a good π -acceptor ligand (carbene) and on the lower frequency side when the unique ligand is a poor π -acceptor ligand (amine).

The IR spectra for complexes **1** and **2** were recorded in hexane; the A_1^1 , A_1^2 , B_1 and E bands can easily be identified as observed in Figure 2.10. The pattern and intensities of bands are characteristic for a $M(CO)_5$ fragment of an octahedral complex.

The wavenumbers of the carbonyl bands for compounds **1** and **2** lie between 2128 and 1718 cm^{-1} , which indicates the presence of terminal carbonyl groups only.

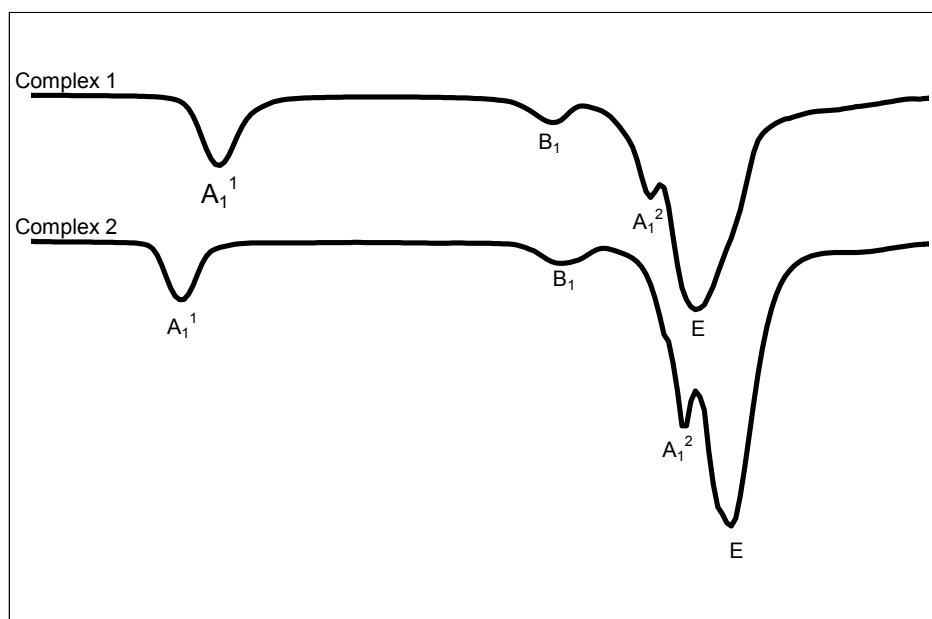


Figure 2.10 Stacked infrared spectrum of compounds **1** and **2** in the carbonyl region

Table 2.3 IR-data^a in the carbonyl region of complex **1** and **2**

Complex	Carbonyl vibrating frequencies (ν_{CO} , cm^{-1})			
	$A_1^{(1)}$	B_1	$A_1^{(2)}$	E
1	2058m	1984w	1959s	1948vs
2	2067m	1981vw	1955s	1945vs

^aHexane as solvent

3.3 X-ray Crystallography

Final confirmation of the structures of **1** and **2** was obtained from single crystal X-ray diffraction studies. The complexes were crystallised from a layered 1:1 dichloromethane:hexane solution. This method gave dark red-brown crystals of good quality for both complexes. Figures 2.11 and 2.12 represent the ORTEP¹⁷ + POV-Ray¹⁸ plots of the geometry of **1** and **2**, which also indicate the atom numbering scheme that was used for the structural data. Compound **1** crystallized in the space group P 21/m with $a = 9.2928(11)$, $b = 7.6330(9)$, $c = 12.4413(15)$ Å, $Z = 2$, compound **2** also crystallized in the space group P 21/m with $a = 9.3964(6)$, $b = 7.7430(5)$, $c = 12.5316(7)$ Å and $Z = 2$. The most important bond lengths and angles are listed in Table 2.4, whilst the most important

torsion angles are listed in Table 2.5. Other structural information is captured on the supplementary CD.

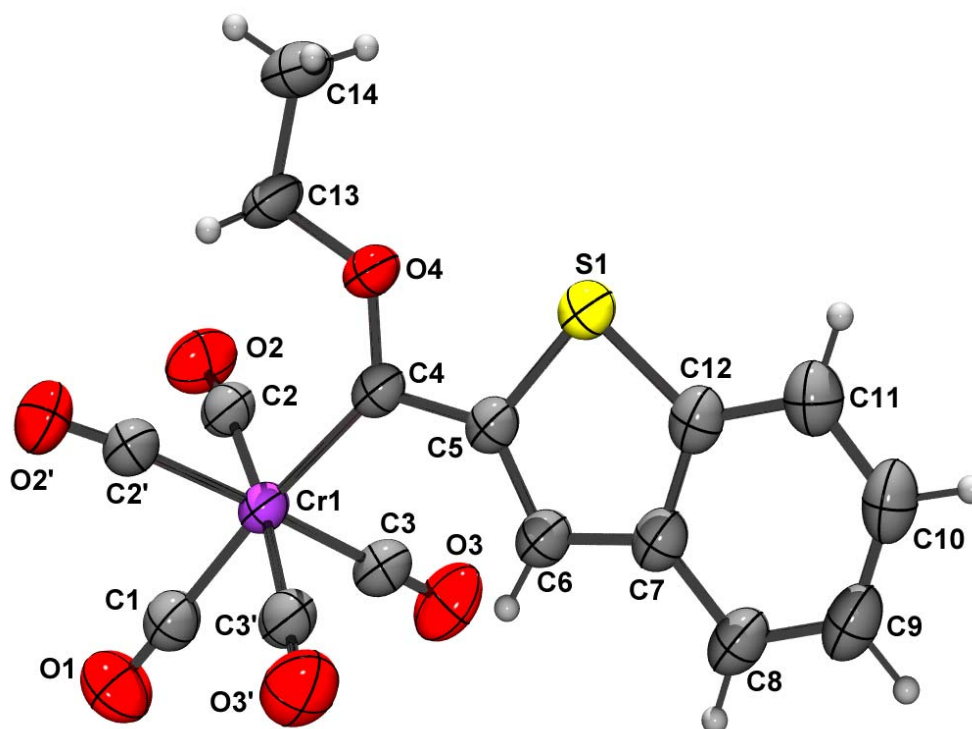


Figure 2.11 ORTEP + POV-Ray plot of the geometry of complex 1

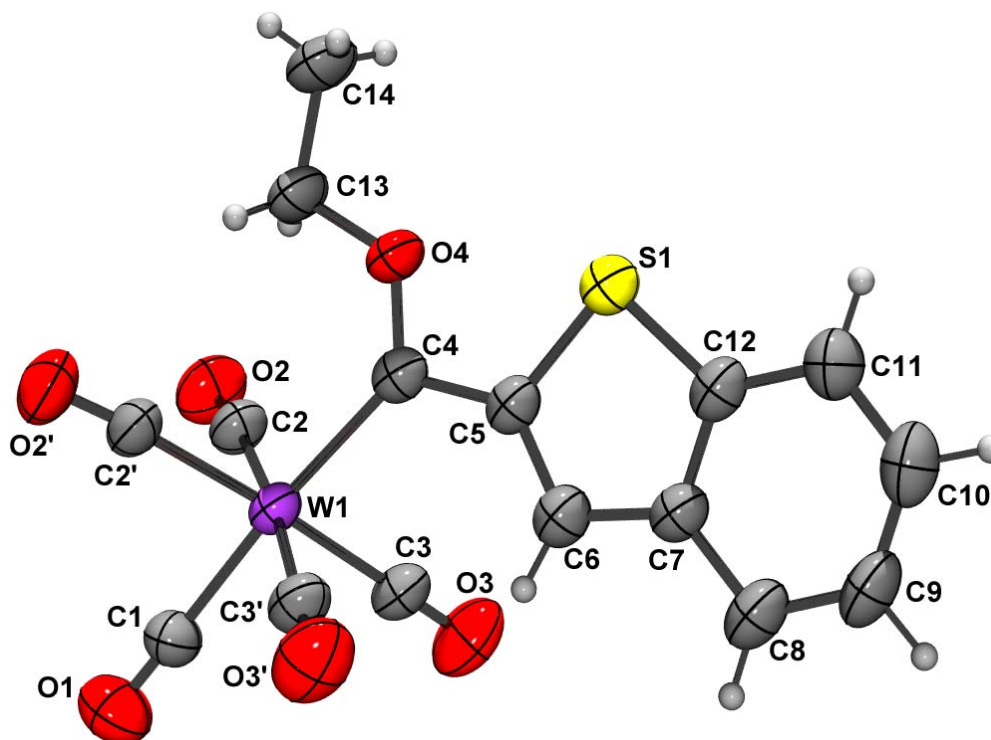


Figure 2.12 ORTEP + POV-Ray plot of the geometry of complex 2

Table 2.4 Selected bond lengths and angles of **1** and **2**

Bond	Bond Lengths (Å)		Bond	Bond angles (°)	
	1 (M = Cr)	2 (M = W)		1 (M = Cr)	2 (M = W)
M(1)-C(4)	2.067(3)	2.201(5)	C(1)-M(1)-C(4)	175.08(10)	175.01(19)
C(4)-O(4)	1.319(3)	1.315(6)	O(4)-C(4)-C(5)	105.2(2)	105.7(4)
C(4)-C(5)	1.462(3)	1.468(7)	O(4)-C(4)-M(1)	129.92(17)	130.1(4)
O(4)-C(13)	1.449(3)	1.448(6)	C(5)-C(4)-M(1)	124.89(17)	124.2(4)
M(1)-C(1)	1.875(3)	2.018(6)	C(4)-O(4)-C(13)	123.3(2)	122.3(4)
M(1)-C(2,2',3,3') ^a	1.9044(19)	2.036(4)	C(4)-C(5)-S(1)	119.52(18)	119.4(4)
C(5)-C(6)	1.368(3)	1.356(7)			
C(6)-C(7)	1.421(4)	1.426(7)			
C(7)-C(12)	1.399(4)	1.403(7)			
C(12)-S(1)	1.727(3)	1.733(5)			
C(5)-S(1)	1.758(3)	1.757(5)			

^a mean value**Table 2.5** Selected torsion angles of **1** and **2**

Bond	Torsion angle (°)	
	1 (M = Cr)	2 (M = W)
C(2)-M(1)-C(4)-O(4)	44.17(6)	43.97(11)
M(1)-C(4)-O(4)-C(13)	0.0	0.0
O(4)-C(4)-C(5)-S(1)	0.0	0.0
M(1)-C(4)-C(5)-S(1)	180.0	180.0

Structural information shows that complexes **1** and **2**, in the solid state, have nearly octahedral geometries of ligands surrounding the metals. A mirror plane, with the carbene ligand in the plane, bisects two sets of carbonyls in the equatorial plane. This can be seen by looking at torsion angles C(2)-M(1)-C(4)-O(4) (**1** = 44.17(6), **2** = 43.97(11)) and C(2)-M(1)-C(4)-C(5) (**1** = -135.83(6), **2** = -136.03(11)). In both complexes two of the equatorial carbonyls bend away from the carbene carbon towards the trans carbonyl as seen by looking at angles C(2)-M(1)-C(4) (**1** = 96.37(7), **2** = 96.52(15)) and two bend towards the carbene ligand as seen by angles for C(3)-M(1)-C(4) (**1** = 87.98(7), **2** = 88.06(15)).

For complexes **1** and **2** the sulphur atom of the thiophene ring is on the same side as the oxygen atom of the ethoxy substituent, indicating restricted rotation around the C4-C5 bond or a preferred packing order in the solid state. This may be as a result of the stabilization of the metal acylate by a five membered ring containing the lithium ion in close contact to the hetero atoms as seen in Figure 2.13.

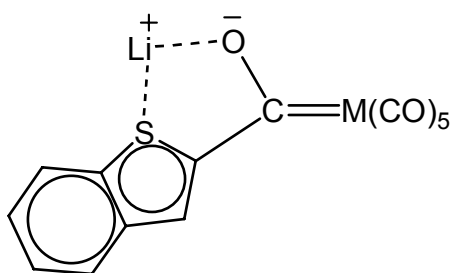


Figure 2.13 Proposed stabilization of the metal acylate

M=C(carbene) distances for alkoxy carbene complexes with two alkyl or aryl substituents are between 2.00 and 2.13 Å for [Cr(CO)₅(carbene)] and 2.15 and 2.25 Å for [W(CO)₅(carbene)].¹⁹ Distances for **1** and **2** fall within these ranges and are comparable with a distance of 2.053(1) Å for [Cr(CO)₅{C(OEt)}Me] and 2.221(8) Å for [W(CO)₅{C(OEt)thienothiophene}].²⁰ The Cr-C(carbene) distance of 2.067(3) Å for **1** is significantly shorter than a Csp²-Cr single bond distance of 2.21(2) Å showing metal to carbene carbon back-bonding.²¹

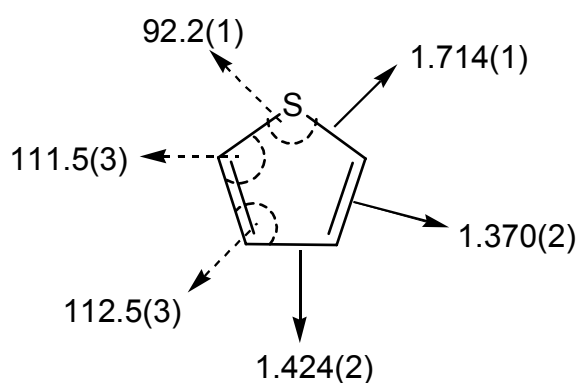


Figure 2.14 Bond lengths (Å) and bond angles (°) of free thiophene²²

When comparing the bond lengths for the carbene substituents of **1** and **2**, the following conclusions can be made:

- (i) The C(4)-O(4) distances are around 1.317(4) Å for **1** and **2**, which is significantly shorter than a Csp^2 -O single bond distance of 1.336 Å, typical for organic esters.
- (ii) The C(carbene)-C(thienyl) bond (Cr : 1.462 Å) is slightly shorter than a distance of 1.48 Å accepted for a Csp^2 - Csp^2 single bond. The distances in the thiophene rings of **1** and **2** are very similar to those in a free thiophene ring and represent a similar degree of delocalization in **1** and **2**.
- (iii) Significant, however is the much shorter C-S distances (1.714(1) Å) in free thiophene compared to the corresponding distances of BT in **1** and **2**.

In summary, delocalization of electron density in the thiophene ring remains more or less the same for the carbon atoms, but is disrupted to the sulphur and spills over to the carbene carbon.

4. References

1. E.O.Fischer, A.Maasböl, *Angew. Chem.* **1964**, 76 645.
2. R.Aumann, E.O.Fischer, *Chem. Ber.* **1968**, 101 954.
3. T.M.Krygowski, M.K.Crañski, Z.Czarnocki, G.Häfelinger, A.R.Katritzky, *Tetrahedron* **2000**, 56 1783.
4. P.Geneste, A.Guicla, D.Levaché, *Bull. Chem. Soc. Fr.* **1983**, 5-6 136.
5. J.A.Connor, E.M.Jones, E.W.Randall, E.Rosenberg, *J. Chem. Soc., Dalton Trans.* **1972**, 2419.
6. O.S.Mills, A.D Redhouse, *J. Chem. Soc. A* **1968**, 3 642.
7. E.O.Fischer, E.Moser, *J. Organomet. Chem.* **1968**, 15 157.
8. J.A.Connor, E.M.Jones, *J. Chem. Soc. A* **1971**, 1974.
9. Y.M.Terblans, H.M.Roos, S.Lotz, *J. Organomet. Chem.* **1998**, 566 133.
10. E.O.Fischer, W.Held, F.R.Kreissl, A.Frank, G.Huttner, *Chem. Ber.* **1977**, 110 656.
11. K.D.Bartle, R.S.Matthews, D.W.Jones, *Tetrahedron* **1971**, 27 5177.
12. P.D.Clark, D.F.Ewing, R.M.Scrowston, *Org. Magn. Reson.* **1976**, 8 252.
13. R.Meyer, S.Brink, E.J.van Rensburg, G.K Jooné, H.Görls, S.Lotz, *J. Organomet. Chem.* **2005**, 690 117.
14. F.H.Köhler, H.J.Kalder, E.O.Fischer, *J. Organomet. Chem.* **1975**, 85 C19.
15. C.Elsenbroich, A.Salzer, *Organometallics: A Concise Introduction*, VCH Verlagsgesellschaft, Weinheim, Germany **1992**, p. 227.
16. L.M.Haines, M.H.B.Stiddard, *Adv. Inorg. Chem. Radiochem.* **1969**, 12 53.
17. L.J.Farrugia, *J. Appl. Crystallogr.* **1997**, 30 565.
18. The POV-Ray Team, POV-Ray 2004 . URL: <http://www.povray.org/download/>.
19. K.H.Dötz, H.Fischer, P.Hofmann, F.R.Kreissl, U.Schubert, K.Weiss, *Transition metal carbene complexes*, (VCH Verlag Chemie) Weinheim **1983**.
20. M.Landman, Synthesis of metal complexes with thiophene ligands, PhD thesis, University of Pretoria **2000**, p86.
21. J.A.Connor, O.S.Mills, *J. Chem. Soc.A* **1969**, 334.
22. J.Chen, L.M.Daniels, R.J.Angelici, *Polyhedron* **1990**, 9 849.